Available online at www.sciencedirect.com
ScienceDirect
Journal of Power Sources 158 (2006) 920–926
JOURNAL OF POWER SOURCES
www.elsevier.com/locate/jpowsour

Corrosion of low-antimony lead–cadmium alloys in conditions of long-term polarization

Alex Nuzhny *

Vlader Enterprise Ltd., 253rd km, UA-61109, Kharkov, Ukraine

Available online 15 December 2005

Abstract

Nowadays, lead-acid battery grids are manufactured mostly from low-antimony and lead–calcium alloys. A variable corrosion resistance of battery grids is caused by either battery operation conditions, purity of used alloy components, an alloy makeup, and the castings quality. Such compositions as usual lead–antimony alloy, low-antimony lead–arsenious alloy and lead–calcium alloy with moderate content of tin today may be regarded as the most studied ones. A significant share of published works has been devoted to low-antimony lead–tin alloys. In the present article, results of corrosion tests of the samples made with application of cadmium as the second component of low-antimony alloy, has been represented. Several samples were extra-alloyed by selenium and silver. Samples of lead–calcium and usual antimony alloys as well as pure lead samples were being tested simultaneously. Upon termination of polarization, weight of anodic films referred to a unit of the sample surface has been determined. Thus, the film covering lead–antimony alloy sample has the maximal weight, whereas the oxidation products on the pure lead surface have the lowest one. Among low-antimony alloys, the highest corrosion resistance has been found out with the samples alloyed by a low amount of silver. The microstructure of the castings surface has been analysed. Process of corrosion has been considered in connection with size of grains.

Keywords: Lead-acid batteries; Low-antimony alloys; Cadmium; Microstructure; Corrosion; Anodic oxidation

1. Introduction

Recently, scientific and technical literature has been focusing attention onto the problem of corrosion of lead-acid battery grids in conditions of continuous operation. Among the published works there have been some articles devoted to the theme of corrosion both low-antimony and lead–calcium alloys, and in this sense the well-known compositions like Pb–Sb–Sn and Pb–Sb–(As)–(Sn) should be considered the most popular ones [1–3]. The last alloy containing tin and arsenic in small amounts as well as the usual antimony–lead alloy containing 5–7 wt.% of antimony has been the most investigated material for battery grids manufacturing. The arsenious alloys are yet not free from some drawbacks: they are inclined to cracking at storage; antimony content in such alloys may be lowered only up to a certain limit.

Low-antimony alloys containing cadmium as the second component, whose content is nearly equal to that one of antimony, have to be allocated into a separate group. In press there is some information regarding studying properties of the above alloys [4–7]. One of the appreciable differences in properties is significant ductility of a casting even after long ageing. A high hardening rate after moulding has also to be attributed to doubtless advantages of these alloys [6]. However, certain drawbacks are inherent to Pb–Sb–Cd alloys: in particular, certain instability of a melt when no preventive measures, because of a high vapour pressure above liquid cadmium.

2. Experimental

2.1. Samples preparation

To carry out the experiment, samples of the alloys being tested for loss of weight at long-term anodic polarization were cast at 180–190 °C into a water-cooled divided slot mould. The mould inside has been covered by a cork-based heat-insulating coat. Time of casting detention in the mould was 8–10 s; the melt was heated up to 380–390 °C. Then rectangular samples of the size 14.4 cm × 2.5 cm were cut out from the obtained castings. Linear dimensions of the samples were measured with accuracy

* Present address: ul. Bakulina 3-72, UA-61166, Kharkov, Ukraine. Tel.: +38 057 7174358/7024084; fax: +38 057 7174358.
E-mail addresses: vladar2001@mail.ru, onk@interami.com.

0378-7753/$ – see front matter © 2005 Elsevier B.V. All rights reserved.
doi:10.1016/j.jpowsour.2005.11.012

Table 1
The anodes makeup (wt.%)

Alloy	Sb	Cd	Ag	Se	Sn	Ca
Pb	–	–	–	–	–	–
Pb–Sb	5.51	–	–	–	–	–
Pb–Sb–Cd	2.04	2.21	–	–	–	–
Pb–Sb–Cd–(Se)	1.91	1.96	–	0.08	–	–
Pb–Sb–Cd–(Se)–(Ag)	1.89	1.97	0.04	0.05	–	–
Pb–Sn–Ca	–	–	–	–	1.05	0.16

of 0.1 mm, thickness—with accuracy of 0.01 mm. After the measurements had been carried out, the prepared samples were carefully degreased, and then weighed on analytical balance to within 0.0001 g. Subsequently, these samples serve as anodes in the electrochemical cells.

Cathodes were made of high-purified lead (>99.98 wt.%) by moulding in a slot mould of the same configuration, as at the anodes casting. Both the moulding modes and the castings detention in the mould were similar to the corresponding parameters at the anodes moulding. Geometrical shape of the cathodes was within 0.4% to the anodes one.

2.2. Testing procedure

The essence of the experiment has lain in a long-continued anodic oxidation of various alloys samples under galvanostatic conditions and in the followed gravimetric finding of the anodes weight losses through the oxidation. The samples elementary makeup determined by means of the chemical analysis has been listed in Table 1.

Each electrochemical cell consisted of four cathodes and three anodes positioned serially on an identical distance from each other. Pure lead served as a material of anodes in the sixth cell; bismuth content in them did not exceed 0.011 wt.%. Three hundred cubic centimeters of sulphuric acid solution having density 1.280 g cm^{-3} at 20 °C was entered into each cell. The electrolyte was prepared of pure sulfuric acid and deionized water whose conductivity did not exceed 5×10^{-6} S cm^{-1}. The whole electrodes surface was under the electrolyte level in the cell, the only lug area not being immersed. Thus inaccuracy of the measurement has been minimized. The cells were incorporated in succession; electric communications provided minimal current losses in joint positions of current carrying parts. Further, the samples were being undergone polarization in galvanostatic conditions within 20 days (480 h). Total quantity of electricity past through a cell has made 72 A h. Both constant temperature of electrolyte (21 ± 1 °C) and invariable current density (8.2×10^{-4} A cm^{-2}) were being maintained through the testing. Density of electrolyte was being maintained also to be constant, and its value was 1.282 ± 0.002 g cm^{-3} (at 20 °C). As soon as polarization has terminated, the samples had been washed in distilled water, and formed anodic films were removed in a solution consisting of sodium hydroxide (160 g dm^{-3}) and sugar (200 g dm^{-3}). Hydrogen peroxide often used in solutions intended for PbO_2 removing from electrodes surface was not applied to prevent from an oxide layer appearance just after removal lead dioxide. Solutions containing sodium thiosulphate or hydrazine salts were not applied due to long-continued reduction and probable incompleteness of removal of an anodic film. The washed and dried samples were weighed on analytical balance to within 0.0001 g. Results of the weighing have been submitted in Table 2. The average value of results of three samples weighing was considered as the weight loss for the alloy. The found weight of the anodic film was referred to the sample surface immersed into electrolyte. Diagram in Fig. 1 shows weight losses of 1 cm^2 of various alloys samples surface for 24 h of polarization.

While testing, potentials of half-cells with diffusive potential elimination were being measured by means of a silver chloride reference electrode. To prevent influence of chloride-ions on the potential value, a salt bridge was used in the measurements. Its cavity was filled up with electrolyte from a cell. The measuring span was 20–24 h; values of daily average potential have been listed in Table 3. Anode potential equalization has occurred within 1–2 days since the polarization started, depending on a tested alloy.

Table 2
Summary weight losses of the exposed samples after the treatment

Alloy	Weight losses (mg cm^{-2})			
	Samples			Average value
Pb–Sb	28.16	27.94	26.68	27.59
Pb–Sb–Cd–(Se)	20.72	20.68	19.68	20.36
Pb–Sb–Cd	18.68	18.18	17.96	18.27
Pb–Sn–Ca	14.68	15.24	13.68	14.53
Pb–Sb–Cd–(Se)–(Ag)	13.08	13.64	12.86	13.19
Pure lead	12.88	13.04	13.00	12.97

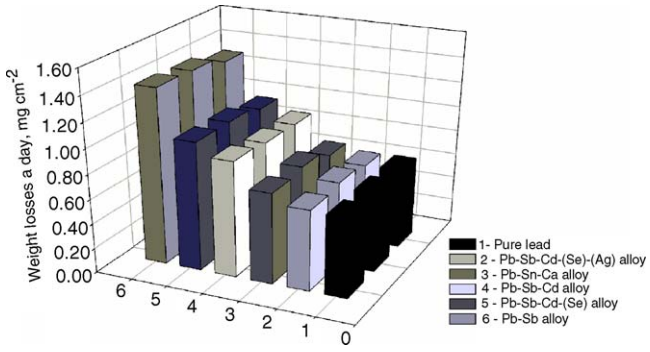

Fig. 1. Weight losses of the exposed samples after anodic polarization.

Table 3
Mean daily positive electrode potential referred to the hydrogen electrode at 22 °C

Alloy	E (mV)
Pb–Sb	1633
Pb–Sb–Cd–(Se)	1658
Pb–Sb–Cd	1664
Pb–Sn–Ca	1676
Pb–Sb–Cd–(Se)–(Ag)	1628
Pure lead	1682

3. Microstructure of the samples

The alloys samples surface was investigated by means of a scanning electronic microscope (SEM) both before the polarization startup and just after its termination. Before the observations were carried out, the castings had been aged within 8–10 days at room temperature to allow recrystallization to be completed. Several samples, as will be noted in Section 3.1, were exposed to etching for uncovering the structure of a surface.

3.1. As-cast samples surface

As seen in Figs. 2 and 3, the samples cast of pure lead show moderately smooth, not porous surface even at a substantial magnification. To uncover structure of lead–calcium alloy surface, a fluorine-content etchant had to be used for removing the aluminium oxide layer from the sample (Figs. 4 and 5).

The structure of low-antimony lead–cadmium alloys surface doped by selenium is shown in Figs. 6 and 7, where the first of them also contained an increased amount of silver. Even

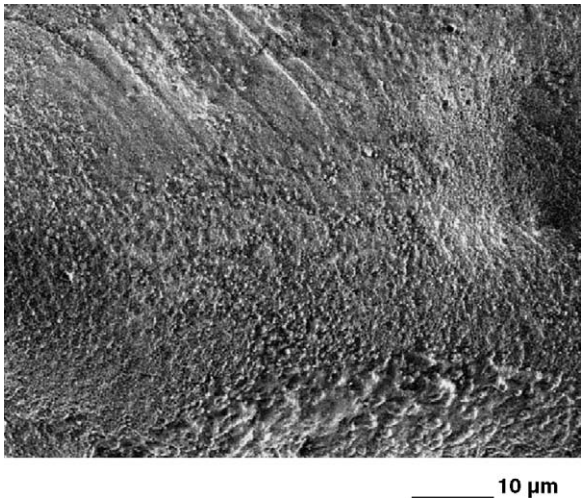

Fig. 2. The etched pure lead sample before testing.

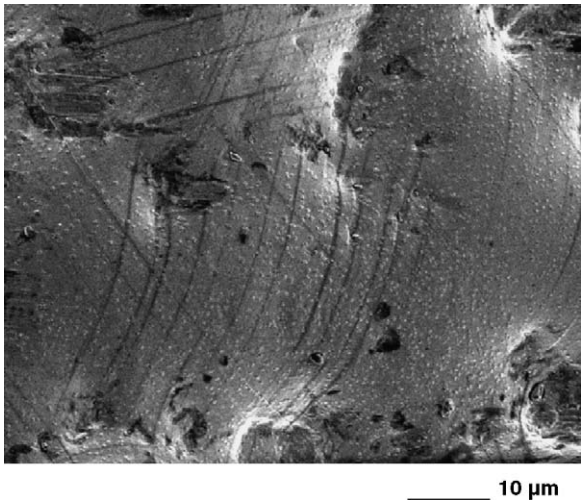

Fig. 3. The pure lead sample before testing.

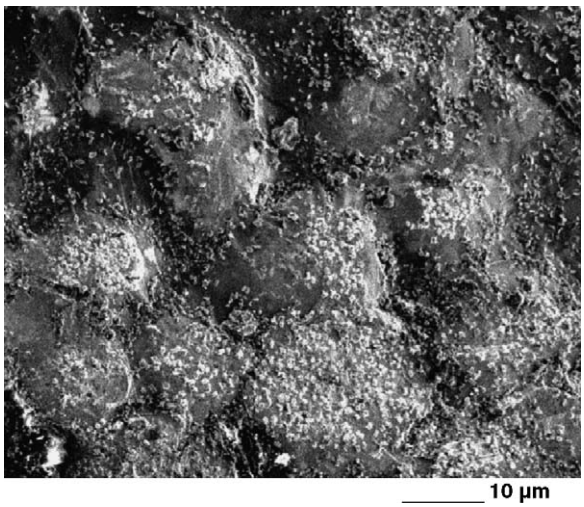

Fig. 4. The etched Pb–Sn–Ca sample before testing.

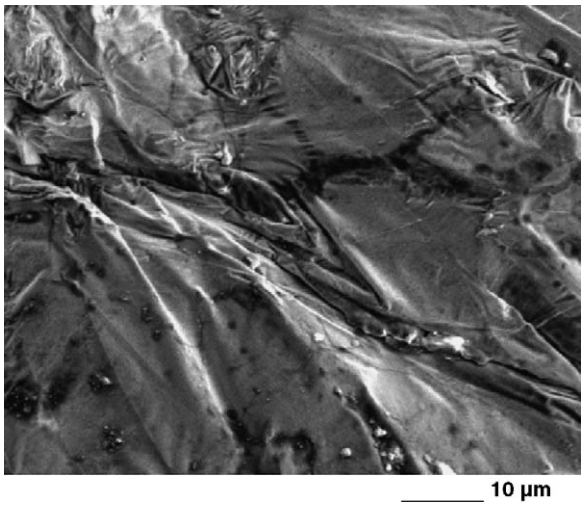

Fig. 5. The Pb–Sn–Ca sample before testing.

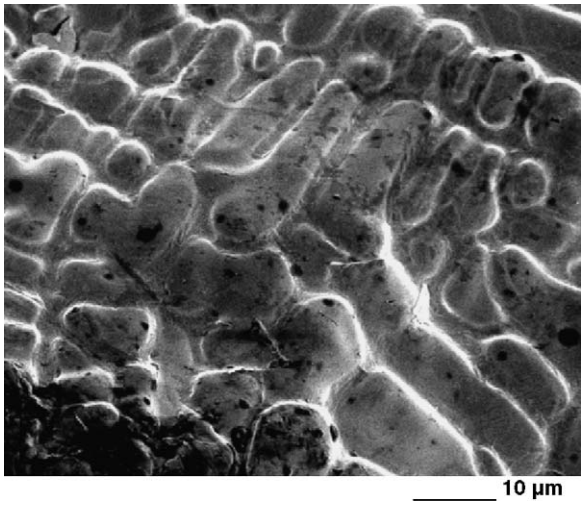

Fig. 6. The Pb–Sb–Cd–(Se)–(Ag) sample before testing.

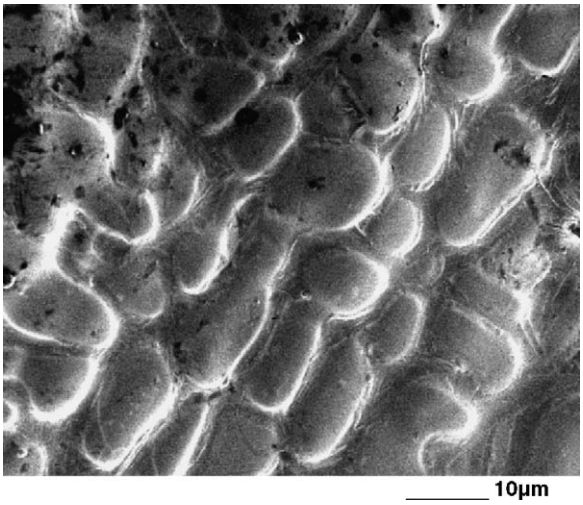

Fig. 7. The Pb–Sb–Cd–(Se) sample before testing.

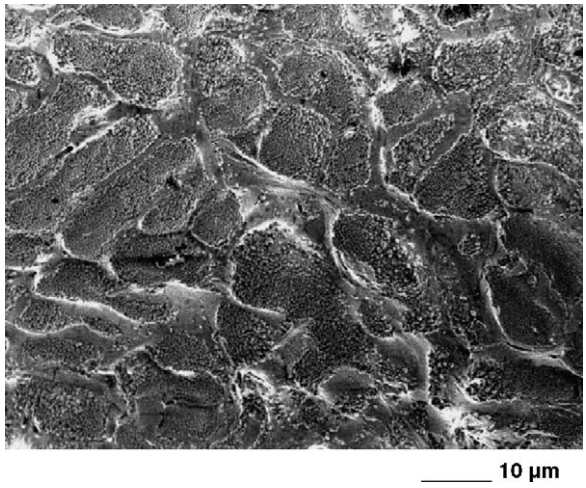

Fig. 8. The etched Pb–Sb–Cd sample before testing.

without a chemical treatment of a sample, essential distinction in size of grains can be recognized in the researched alloys. The silver-containing alloy has more fine-grained and homogeneous structure; dispersion of the grain size in comparison with Pb–Sb–Cd–(Se) alloy is rather low. The substantial discrepancy in properties of makeup-similar alloys doped by silver may be clarified by appearance of a new compound in the alloy. An example of such compound is silver selenide—a substance that is rather stable thermodynamically ($\Delta H_f^\circ \approx 26\,\mathrm{kJ\,mol^{-1}}$). β-$Ag_2Se$ modification existing at temperature higher than 133 °C is isomorphic to lead, hence its increased solubility in lead should be expected in liquid state. A mention of silver selenide influence on crystal structure of lead alloys is given in [8]. Silver does not form any compound with lead; at insignificant Ag content the binary system Pb–Ag is of a hypoeutectic type [9, v. 1, p. 71], whereas in system Pb–Se there is the only PbSe substance melting congruently at 1080.7 °C [9, v. 3, pp. 789–791]. At the moulding temperature (390 °C) solubility of selenium in liquid lead is low enough and makes up 0.026% (mol). If doped by cadmium, CdSe compound may be expected to occur in the alloy. At 317 °C, this compound forms a degenerate eutectic with cadmium excess [9, v. 1, pp. 873–874].

Thus, the formation mechanism of fine-grained structure of Pb–Sb–Cd–(Se)–(Ag) alloy is associated with the existence of two compounds in the system: β-Ag_2Se and known intermetallide CdSb formed in low-antimony lead–cadmium alloys. The last compound melts congruently in a metastable state at 390 °C, i.e. at the temperature close to usual modes of moulding. Particles of silver selenide that appear in the melt at casting cooling can serve as the nucleation sites of CdSb compound. With regard to both temperature of the poured melt (390–420 °C) and melting temperature of the above compound, duration of this intermetallide crystallization at casting solidification should not be too long-term. Hence, to achieve a good crystal structure of a grid, Ag/Cd molar ratio 2/1 or 2.73/1.00 (wt.) should be recommended. The well-detailed structure of a casting surface that contacts directly with the mould inside (Fig. 6) should be clarified by uniform heterogeneous crystallization in space. In Figs. 8 and 9 structure of the sample surface cast from Pb–Sb–Cd alloy, which was alloyed neither by selenium nor by silver, is shown. Attention should be paid to the circumstance that in this case preliminary etching of a sample is required to uncover crystal structure because isolation of grains from a surface is not obviously expressed. Probably, it may be associated with the circumstance that the surface of casting at its solidification is being covered with a thin layer of a liquid phase enriched with lead. The more the essential difference of Sb/Cd ratio as against the equimolar one, the lower the temperature of crystallization of this liquid phase. Thus, when extraneous impurities being absent, there are two phases in shape at melt solidification for a rather long time, that may produce a columnar structure of a grid, and shrinkage cracks may occur at excessive detention. Deactivation of nuclei may be generated, first of all, either by the mould surface temperature increase or insufficient heat removal from the grid surface.

As it was pointed out above, Pb–Sb–Cd–(Se) alloy is an example of a composition that fills an intermediate place on crystal structure of a casting. It should be supposed that nucleation process begins on CdSe particles that appear in melt at

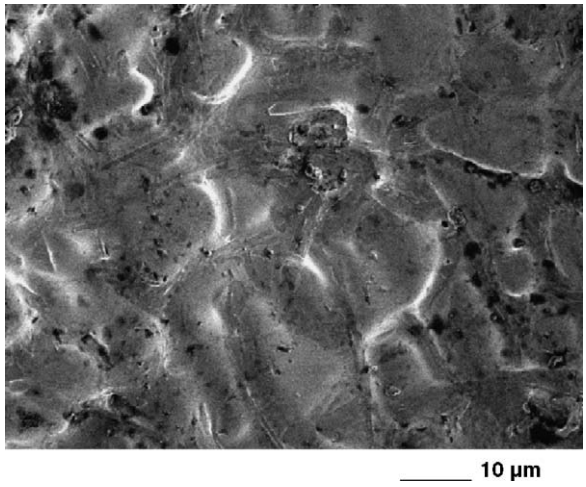

Fig. 9. The Pb–Sb–Cd sample before testing.

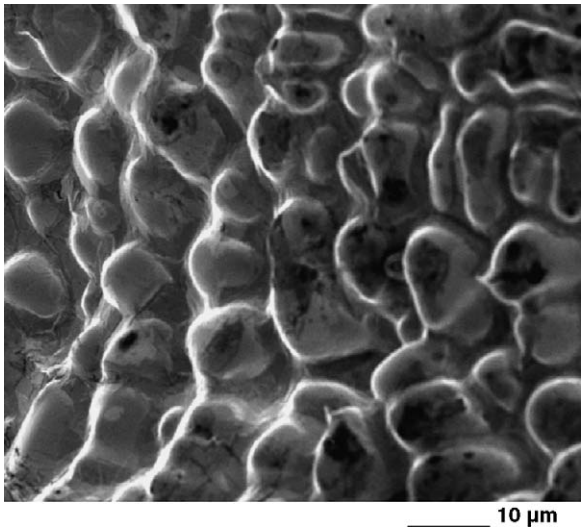

Fig. 10. The Pb–Sb sample before testing.

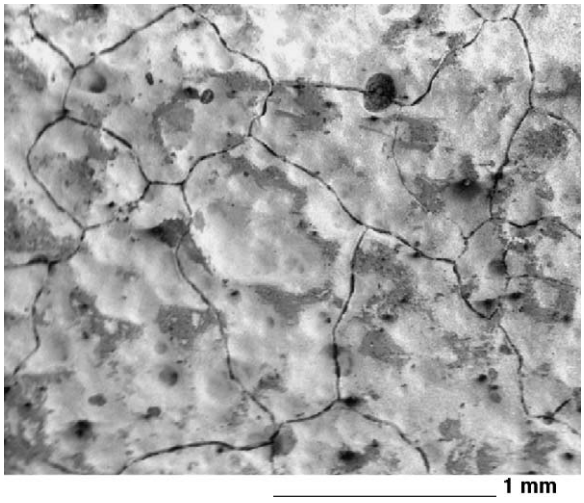

Fig. 11. The corroded pure lead sample.

casting solidification. As recognized in Fig. 7, segregate structure of the casting surface has been expressed less obviously that should be associated with the existence of a ternary peritectic $Cd_xSb_ySe_z$ phase of unstochiometric structure enriched with cadmium on the grains boundaries.

Fig. 10 shows the structure of a surface of the sample cast of usual antimony alloy. One can observe that both linear dimensions and shape of the grains do not differ substantially as compared to the similar formations in lead–cadmium alloys. The single appreciable distinction of the segregate pattern of antimony alloy is the isolation of grains from the casting surface expressed obviously.

3.2. Surface of the samples after anodic oxidation

On having the testing terminated, the samples surface was repeatedly re-examined on SEM. Cellular structure typical for pure lead, which has not been uncovered on the samples up to undergoing polarization (Figs. 2 and 3), has been shown in Fig. 11. Fig. 12 demonstrates the same sample surface at a greater magnification. The increase in the surface active area, caused by eroding of grain boundaries owing to segregate phase oxidation, tends to zero in this case. A cellular indendritic structure with increased grains size can be recognized on the surface of Pb–Sn–Ca alloy sample (Fig. 13). As it can be seen in the picture, corrosion of the material is superficial enough and does not substantially penetrate into the casting; hence, the active surface area increases quite insignificantly.

The view of the samples surface shown in Figs. 14–15 allows evaluating distinction of a castings surface of lead–cadmium alloys, which in addition have been doped by both selenium, and selenium and silver. On the surface of Pb–Sb–Cd–(Se)–(Ag) alloy sample a linearly ordered structure is recognized, where dendritic nature of grains is expressed extremely insignificantly with dominance of the first-order axes. Layers between the grains boundaries are very narrow, so corrosion will not penetrate deeply into a sample and has dot character. Orientation

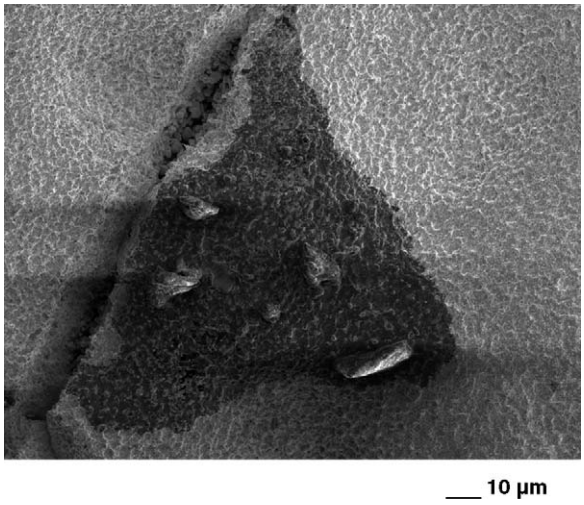

Fig. 12. The corroded pure lead sample.

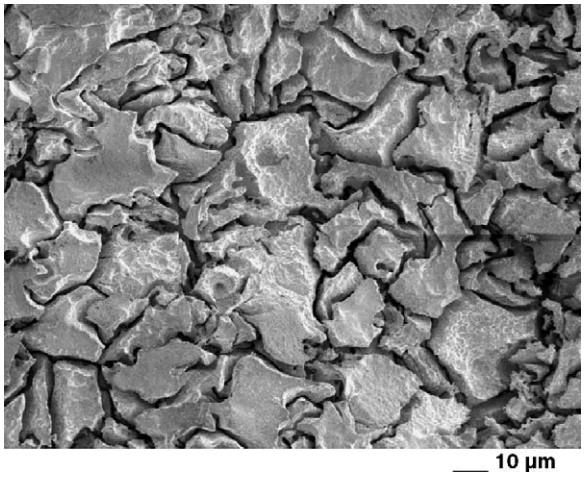

Fig. 13. The corroded Pb–Sn–Ca alloy sample.

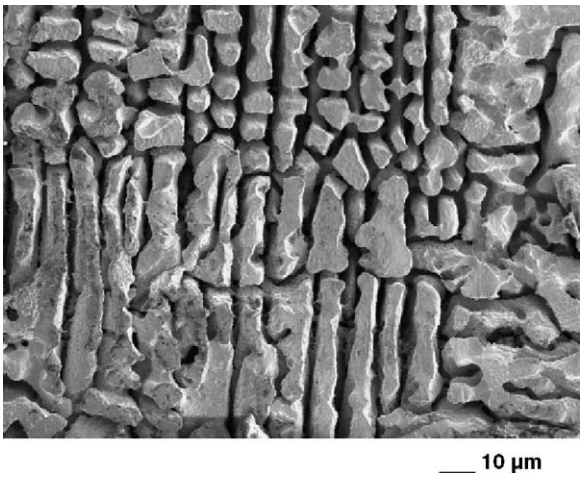

Fig. 14. The corroded Pb–Sb–Cd–(Se)–(Ag) alloy sample.

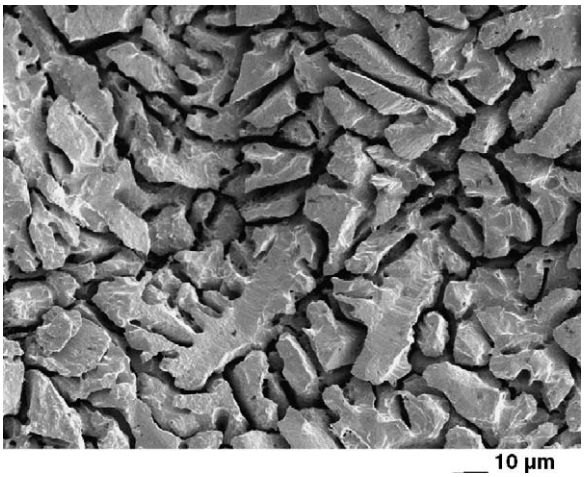

Fig. 16. The corroded Pb–Sb–Cd alloy sample.

of dendrites occurs mainly in one plane arranged athwart to the casting surface. In the absence of silver in the alloy, a positional disorder of rather developed dendrites with the significant linear sizes of second-order axes on the sample surface is recognized (Fig. 15). Three-plane orientation of dendrites along with the significant width of grain boundaries should result in a sharp increase of the surface active area of a sample and, hence, in a porous anodic film appearance.

When analyzing the surface structure of lead–cadmium alloys samples, it should be recognized, that in absence of addition elements the dendrites development is suppressed at the very beginning of their growth (Fig. 16); the width of intergranular layers is less appreciably and on the average does not exceed 4 μm. Erosion of the sample has a superficial and, to some extent, depth character. For comparison, a view of a surface of sample cast of usual antimony alloy has been shown in Fig. 17. The high chemical surface erosion having well-defined depth nature must result in ponderable difference of the visible and active electrode area, that ultimately is one of the principal reasons of increase in anodic film weight.

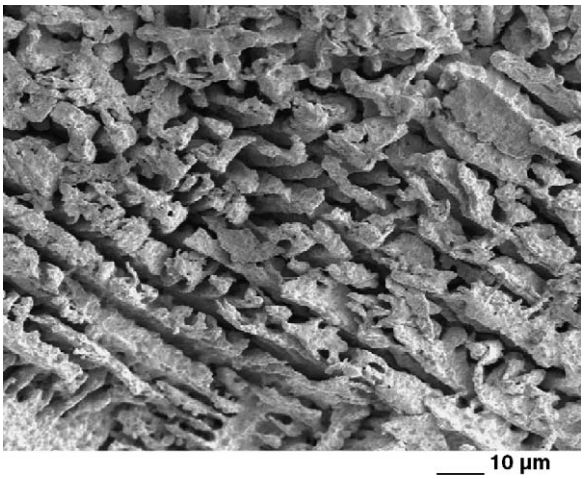

Fig. 17. The corroded Pb–Sb alloy sample.

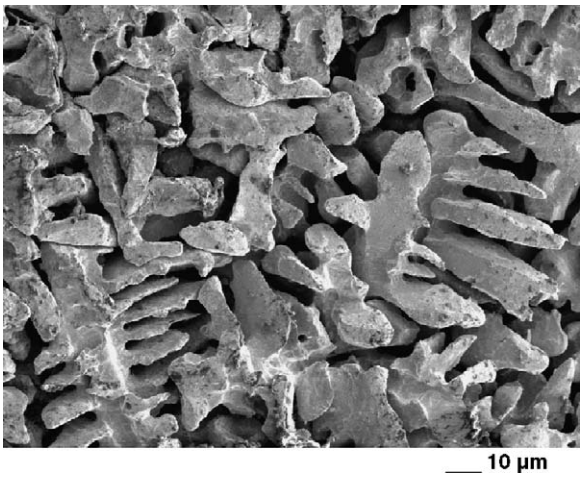

Fig. 15. The corroded Pb–Sb–Cd–(Se) alloy sample.

4. Results

The experiment carried out has resulted in corrosion resistance determination of both low-antimony lead–cadmium alloys and lead–calcium alloy under mentioned conditions of polarization. The findings have been referred to lead–antimony alloy. The values found for corrosion resistance are adduced in Fig. 18. Based on the samples research results that have been ensued by means of SEM, a conclusion must be drawn that corrosion resistance of an alloy depends directly on the active area of grid surface undergoing anodic oxidation. Physical and chemical properties of compounds existing both in the melt and appearing in solidification should be considered as the determining factors. Thus, while Pb–Sb–Cd–(Se)–(Ag) alloy solidifies, Ag_2Se particles are being the nucleating centres of heterogeneous crystallization that results in fine-grained casting structure, which consists of equiaxial crystals segregated with thin intergranular layers. In consequence of a dense anodic film formation, superficial erosion of the sample is low enough. Presence of a highly electropositive element in the alloy makeup results in an

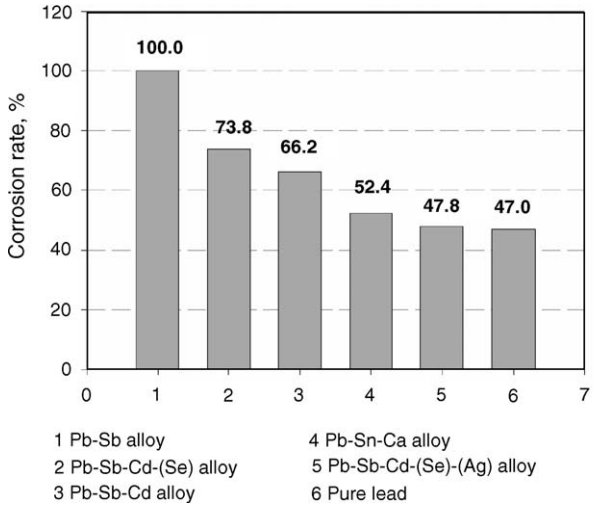

Fig. 18. The tested alloys corrosion resistance referred to lead–antimony alloy.

appreciable decrease in the anode potential when polarizing. Due to the above reasons, corrosion resistance of the alloy is rather significant. On the contrary, Pb–Sb–Cd–(Se) alloy at crystallization forms rather fine-grained structure. However, intergranular layers thickness is substantial enough, so that existence of a hypothetical unstochiometric phase $Cd_xSb_ySe_z$ enriched with cadmium may be presumed. CdSe particles constituting CdSb intermetallide the above-stated ternary phase should be supposed as the initiators of the alloy solidification when cooling. A low value of corrosion resistance of the alloy results from the developed dendritic structure and electrochemical instability of the intergranular cadmium-content phase. Some decrease in daily average potential of the Pb–Sb–Cd–(Se) alloy sample is caused by the presence of an additional electropositive component (Se).

If there are no any alloying components, lead–cadmium alloy reveals a slightly higher resistance to anodic oxidation in comparison with the similar selenium-content alloy. Structure of the Pb–Sb–Cd alloy samples consists of some more coarse grains though the thickness of intercrystalline layers is insignificant. Presence of a superficial layer of a liquid phase enriched with lead at casting solidification makes also a certain contribution into anodic corrosion resistance of a sample, by reason of increased resistance of this layer to electrochemical oxidation in solid state. Corrosion resistance of the alloy is a little bit higher in comparison with that alloyed by selenium.

5. Conclusions

1. Low-antimony lead–cadmium alloy doped by silver and selenium possesses the significant corrosion resistance comparable to pure lead.
2. Influence of selenium on corrosion resistance of Pb–Sb–Cd alloy is insignificant, and under mentioned conditions of polarization, castings of Pb–Sb–Cd–(Se) alloy show some reduction in their resistance to oxidation.
3. Anodic films coating the Pb–Sb–Cd–(Se)–(Ag) samples have appreciably more dense structure and smaller thickness in comparison with those formed on the other tested alloys samples.
4. The increased corrosion resistance of Pb–Sb–Cd–(Se)–(Ag) alloy is clarified, in particular, by size reduction of grains and suppression of development of highly branched dendrites in a casting.
5. Reduction in size of grains and suppression of development of highly branched dendrites in a casting may result in increased corrosion resistance of Pb–Sb–Cd–(Se)–(Ag) alloy.

Acknowledgement

The author is thankful to Dr. Oleg Kalugin, Kharkiv National University, for the SEM observations supply.

References

[1] G.V. Krivchenko, G.N. Gordyakova, K.M. Solovyova, Proceedings of Storage Batteries Research Institute (Rus.), Leningrad, 1980, pp. 3–6.
[2] L.M. Levinzon, I.A. Aguf, M.A. Dasoyan, Proceedings of Storage Batteries Research Institute (Rus.), Leningrad, 1967, pp. 28–35.
[3] M.A. Dasoyan, I.A. Aguf, The contemporary theory of lead-acid cell, (Rus.), Energia, Leningrad (1975) 154–165.
[4] GOULD, Inc., GB Patent 1,427,660 (1976).
[5] G.W. Mao, P. Rao, J.F. Trenter, FR Patent 2,287,782 (1976).
[6] J.F. Trenter, P. Rao, FR Patent 2,489,844 (1980).
[7] G.K. Kasabov, BG Patent 32,937 (1982).
[8] M. Abdel-Reichim, B. Preibisch, W. Reif, Metall 38 (1984) 407–412.
[9] N.P. Lyakishev, The Equilibrium Diagrams of Binary Metal Systems (Rus.), Mashinostroenie, Moscow, 2000.